JBC RESEARCH ARTICLE

Death domain–associated protein DAXX regulates noncoding RNA transcription at the centromere through the transcription regulator ZFAT

Received for publication, June 26, 2022, and in revised form, September 15, 2022 Published, Papers in Press, September 23, 2022,
https://doi.org/10.1016/j.jbc.2022.102528

Shuhei Ishikura[1,2], **Kazumasa Yoshida**[1,2], **Toshiyuki Tsunoda**[1,2], **and Senji Shirasawa**[1,2,*]

From the [1]*Department of Cell Biology, Faculty of Medicine, Fukuoka University, Fukuoka, Japan;* [2]*Research Institute for Advanced Molecular Medicine, Fukuoka University, Fukuoka, Japan*

Edited by Brian Strahl

The centromere is an essential chromosomal structure for faithful chromosome segregation during cell division. No protein-coding genes exist at the centromeres, but centromeric DNA is actively transcribed into noncoding RNA (ncRNA). This centromeric transcription and its ncRNA products play important roles in centromere functions. We previously reported that the transcriptional regulator ZFAT (zinc-finger protein with AT hook) plays a pivotal role in ncRNA transcription at the centromere; however, it was unclear how ZFAT involvement was regulated. Here, we show that the death domain–associated protein (DAXX) promotes centromeric localization of ZFAT to regulate ncRNA transcription at the centromere. Coimmunoprecipitation analysis of endogenous proteins clearly reveals that DAXX interacts with ZFAT. In addition, we show that ectopic coexpression of ZFAT with DAXX increases the centromeric levels of both ZFAT and ncRNA, compared with ectopic expression of ZFAT alone. On the other hand, we found that siRNA-mediated depletion of DAXX decreases the centromeric levels of both ZFAT and ncRNA in cells ectopically expressing ZFAT. These results suggest that DAXX promotes the centromeric localization of ZFAT and ZFAT-regulated centromeric ncRNA transcription. Furthermore, we demonstrate that depletion of endogenous DAXX protein is sufficient to cause a decrease in the ncRNA levels at the centromeres of chromosomes 17 and X in which ZFAT regulates the transcription, indicating a physiological significance of DAXX in ZFAT-regulated centromeric ncRNA transcription. Taken together, these results demonstrate that DAXX regulates centromeric ncRNA transcription through ZFAT.

The kinetochore attaches chromosomes to spindle microtubules in mitosis to segregate each sister chromatid into daughter cells. The centromere is an essential chromosomal structure, in which kinetochore protein complex is assembled, to ensure accurate chromosome segregation (1). The eukaryotic centromeres that lack protein-coding genes had long been thought to be transcriptionally silent regions. However, recent many studies have demonstrated that transcription into noncoding RNA (ncRNA) occurs at the centromeres although the centromeric transcription levels are low (2–6). Centromeric transcription and its ncRNA products have been shown to play crucial roles in centromere functions and kinetochore assembly (7–10). However, there is limited understanding regarding molecular properties of centromeric ncRNA, including nucleotide sequences and transcription regulation.

We have previously reported that the nuclear protein ZFAT (zinc-finger protein with AT hook) plays a pivotal role in ncRNA transcription at the centromere (11–13). ZFAT specifically induces acetylation of lysine 8 in histone H4 at the centromere by recruiting the histone acetyltransferase KAT2B (12). The KAT2B-catalyzed acetylation of lysine 8 in histone H4 at the centromere functions as a binding site for the bromodomain-containing protein BRD4, which stimulates RNA polymerase II–dependent ncRNA transcription (12). ZFAT specifically binds to 8-bp DNA sequences at the centromere, named the ZFAT box (12). Furthermore, we recently reported that the centromeric protein CENP-B interacted with ZFAT to promote the centromeric localization of ZFAT (11).

We have previously demonstrated that ZFAT plays important roles in cell proliferation and survival mainly using mouse (14–19). On the other hand, various studies in human have reported that genetic variants of the *ZFAT* gene are associated with particular human diseases, including autoimmune thyroid diseases (20, 21), aneurysms (22), hypertension (23), and type 2 diabetes mellitus (24). Furthermore, mutations and altered expression of the *ZFAT* gene are also observed in several human cancers (25–30). For example, a genome-wide association study of diffuse large B-cell lymphoma patients showed that specific mutations in the *ZFAT* genes were strongly associated with poorer survival of diffuse large B-cell lymphoma patients (31). Thus, dysregulations of ZFAT function and expression are thought to be related to various human diseases although roles of ZFAT-regulated centromeric transcription in pathogenesis of these diseases are still unknown.

DAXX (death domain–associated protein) is a multifunctional protein involved in many cellular processes, including apoptosis, protein stability, and transcription regulation (32).

* For correspondence: Senji Shirasawa, sshirasa@fukuoka-u.ac.jp.

DAXX itself does not contain any enzymatic catalytic domains, and, thus, functions in these processes through interaction with various molecules. DAXX regulates gene transcription through interaction with various transcription factors. For example, p53 has been identified as a DAXX-interacting protein, and the p53 transcriptional activity is negatively regulated by DAXX (33). On the other hand, Pax5, an essential transcription factor for B-cell development, interacts with DAXX, and their interaction leads to transcription activation in B cells (34). Furthermore, it has been reported that DAXX regulates gene transcription through interaction with histone-modifying enzymes, including the CREB-binding protein (35) and the histone deacetylase 2 (36). Interestingly, through interaction with the chromatin-remodeling protein ATRX (α-thalassemia and mental retardation X-linked), DAXX functions as a histone chaperone for the deposition of histone H3 variant H3.3, which is also related to transcription activation (37). Thus, the dynamic interaction between DAXX and its associated proteins is tightly controlled. Intriguingly, it was previously reported that DAXX was involved in transcription at the centromere through deposition of H3.3 (38). However, the precise mechanisms by which DAXX regulates centromeric transcription remain elusive.

In this study, we show that DAXX interacts with ZFAT to promote centromeric localization of ZFAT, leading to stimulation of ncRNA transcription. Coimmunoprecipitation (co-IP) analyses of endogenous and ectopically expressed proteins clearly reveal that DAXX interacts with ZFAT. Ectopic expression of DAXX increases the centromeric ZFAT levels and stimulates ZFAT-regulated ncRNA transcription at the centromeres. On the other hand, knockdown of DAXX decreases the centromeric levels of ZFAT as well as those of ncRNA. These results indicate that DAXX regulates ncRNA transcription at the centromeres through ZFAT.

Results

DAXX interacts with ZFAT

We previously showed that the centromeric protein CENP-B interacted with ZFAT through its acidic domain (AD) (11). Similar to CENP-B, DAXX is also known as a protein that localizes at the centromeres and contains the AD (32, 39). Therefore, we examined the interaction between DAXX and ZFAT in human embryonic kidney 293 (HEK293) human cells through co-IP analysis using anti-ZFAT and anti-DAXX antibodies. The endogenous ZFAT protein was coimmunoprecipitated with the endogenous DAXX protein using anti-DAXX antibody and vice versa (Fig. 1*A*). These results indicate that DAXX interacts with ZFAT.

To compare an interaction affinity with ZFAT between DAXX and CENP-B, we ectopically expressed hemagglutinin (HA)-tagged ZFAT (ZFAT-HA) and FLAG-tagged DAXX (FLAG-DAXX) or FLAG-tagged CENP-B (FLAG-CENP-B) in HEK293 cells and examined their interaction through co-IP analysis using anti-HA and anti-FLAG antibodies. Similar to endogenous proteins, the FLAG-DAXX protein was coimmunoprecipitated with the ZFAT-HA protein using an anti-HA antibody and vice versa (Fig. 1*B*). The protein levels of ZFAT-HA, which was coimmunoprecipitated with FLAG-DAXX, were relatively lower than those of ZFAT-HA coimmunoprecipitated with FLAG-CENP-B (Fig. 1*B*). Similarly, the protein levels of FLAG-DAXX, which was coimmunoprecipitated with ZFAT-HA, were relatively lower than those of FLAG-CENP-B coimmunoprecipitated with ZFAT-HA (Fig. 1*B*). Furthermore, we examined the interaction between ZFAT and DAXX after DNase treatment through co-IP analysis (Fig. 1*C*). Disappearance of the genome DNA by the DNase treatment was confirmed in our previous study (11). The DNase treatment did not affect the interaction between ZFAT and DAXX. Together, these results suggest that DAXX interacts with ZFAT independently of DNA, and that the interaction affinity between ZFAT and DAXX is slightly weaker than that between ZFAT and CENP-B.

Identification of domains involved in interaction of ZFAT and DAXX

The DAXX protein is composed of several domains, including two SUMO-interacting motifs (SIMs) at the N and C terminus (SIM1 and SIM2, respectively), four helix bundle domains, histone-binding domain, and AD (Fig. 2*A*, (32)). To elucidate DAXX domains involved in the interaction with ZFAT, we examined the interaction between ZFAT-HA and the deletion mutants of FLAG-DAXX in HEK293 cells using co-IP analysis. Deletion of SIM2 hardly affected the interaction with ZFAT, whereas loss of SIM1 slightly decreased it (Fig. 2*B*). Furthermore, deletion of either four helix bundle domain, histone-binding domain, or AD markedly inhibited the interaction of DAXX with ZFAT (Fig. 2*B*). These results suggest that multiple domains of DAXX are involved in the interaction with ZFAT.

The ZFAT protein is composed of 18 zinc-finger (ZF) domains (Fig. 3*A*, (13)). To determine which ZFAT regions were involved in the interaction with DAXX, we evaluated the interaction between FLAG-DAXX and the deletion mutants of ZFAT-HA in HEK293 cells. While the ZF-ΔN-2 deletion mutant, which was composed of ZF9-18, retained the ability to interact with DAXX, the ZF-ΔC-2 deletion mutant, which was composed of ZF1-8, did not interact with DAXX, suggesting involvement of the C-terminal region of ZFAT in the interaction with DAXX (Fig. 3*B*). Furthermore, the interaction with DAXX was clearly observed in the ZF-ΔN-3 deletion mutant, which had ZF13–18 (Fig. 3*B*). These results suggest that the C-terminal region containing ZF13–18 of ZFAT is involved in the interaction with DAXX.

DAXX is involved in the centromeric localization of ZFAT

To elucidate roles of interaction between DAXX and ZFAT in their centromeric localization, we examined the protein levels of ZFAT and DAXX at the centromeres in HEK293 cells, which transiently expressed ZFAT-HA, FLAG-DAXX, or both, using chromatin immunoprecipitation (ChIP)–quantitative PCR (qPCR) analysis that we established previously (11, 12) (Fig. 4, *A* and *B*). We previously showed that ZFAT was bound

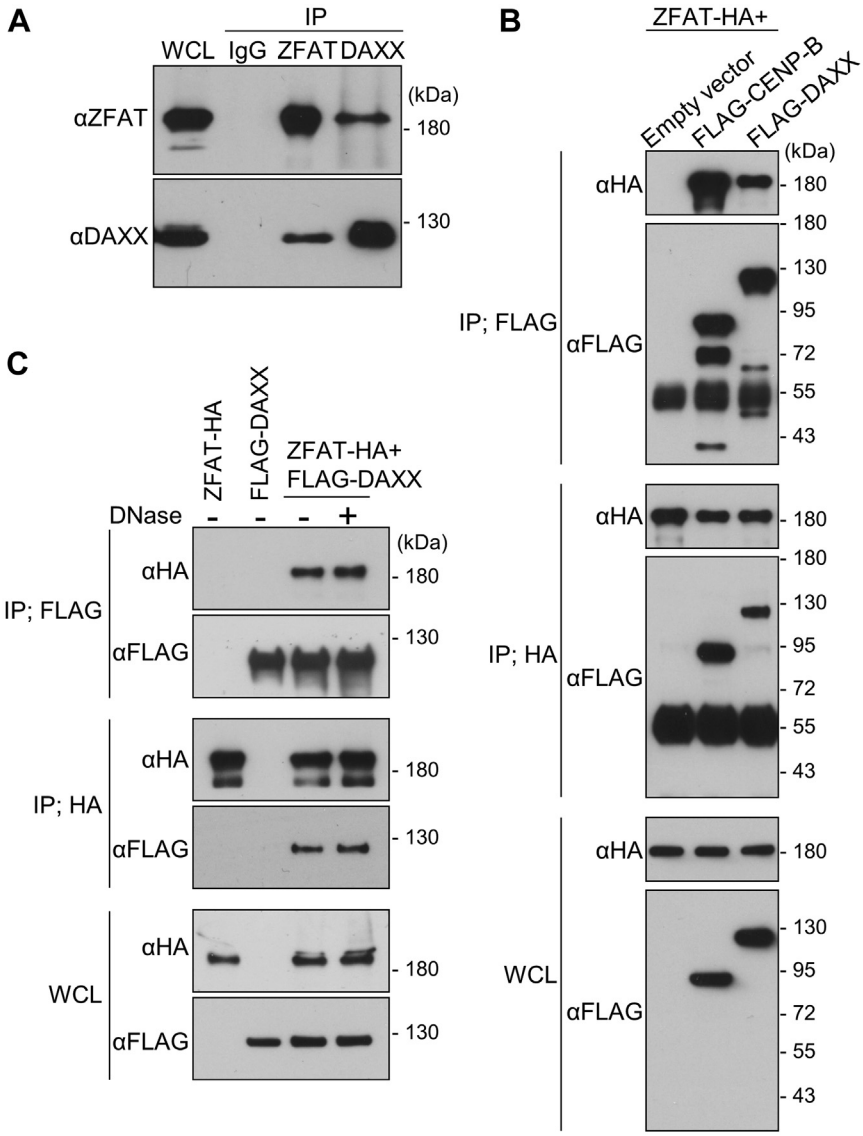

Figure 1. DAXX interacts with ZFAT. *A*, coimmunoprecipitation (co-IP) analysis of endogenous ZFAT and DAXX proteins in HEK293 cells using anti-ZFAT and anti-DAXX antibodies or control immunoglobulin G (IgG). *B*, co-IP analysis of ZFAT-HA and FLAG-CENP-B or FLAG-DAXX using anti-HA and anti-FLAG antibodies in HEK293 cells transfected with the indicated expression vectors. *C*, co-IP analysis of ZFAT-HA and FLAG-DAXX after DNase treatment in HEK293 cells. The data are representative of three independent experiments. DAXX, death domain–associated protein; FLAG-CENP-B, FLAG-tagged CENP-B; FLAG-DAXX, FLAG-tagged DAXX; HA, hemagglutinin; HEK293, human embryonic kidney 293 cell line; WCL, whole cell lysate; ZFAT, zinc-finger protein with AT hook; ZFAT-HA, hemagglutinin-tagged ZFAT.

to the centromeres of every chromosome but regulated the centromeric ncRNA transcription only at particular chromosomes (12). Activation of the centromeric ncRNA transcription by ectopic expression of ZFAT was observed in qRT–PCR analysis using primers for Chr17, and ChrX-a and ChrX-b, but not primers for Chr13/21-a, whereas ZFAT binding at the centromeres was detected in ChIP–qPCR analysis using all these primer sets (12). In the ChIP–qPCR analysis in this study, we used primers for Chr17 and Chr13/21-a to examine whether DAXX was involved in the centromeric localization of ZFAT only at chromosomes where ZFAT activated the ncRNA transcription. We clearly observed that ZFAT-HA and FLAG-DAXX were bound to the centromeres of both Chr17 and Chr13/21, but not to regions for the *5S ribosomal RNA* gene, which were used as a negative control (Fig. 4*B*). Interestingly, ectopic coexpression of ZFAT-HA with FLAG-DAXX further increased the protein levels of ZFAT at the centromeres of both Chr17 and Chr13/21, compared with those in cells expressing ZFAT-HA alone. On the other hand, their coexpression did not affect the protein levels of DAXX at the centromeres, compared with those in cells expressing FLAG-DAXX alone. These results suggest that DAXX plays positive roles in the centromeric localization of ZFAT at every chromosome independently of transcription activation by ZFAT, whereas ZFAT is not involved in the centromeric localization of DAXX. Furthermore, ectopic coexpression of FLAG-DAXX with ZFAT-HA did not affect the ZFAT protein levels at the promoter regions of the *BRPF1*, *PDE12*, and *TELO2* genes to which we previously reported that ZFAT was bound (Fig. 4, *B* and *C*, (15)), suggesting that DAXX is involved in the

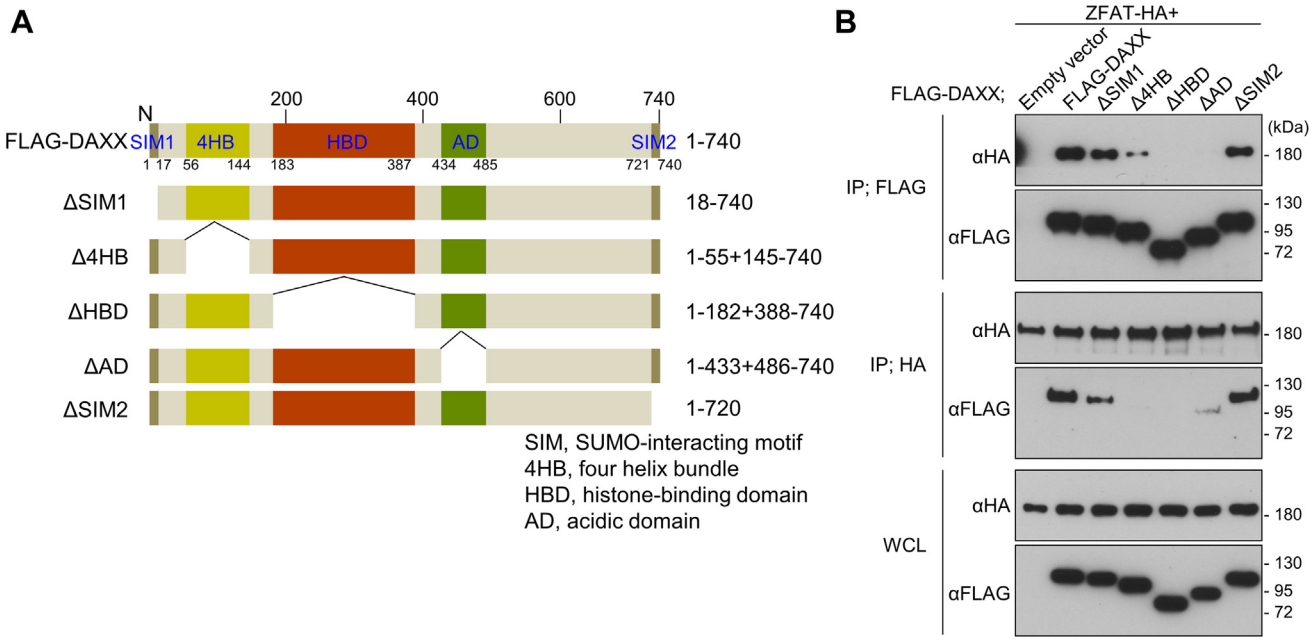

Figure 2. Multiple domains of DAXX are involved in interaction with ZFAT. *A*, schematic diagram of the deletion mutants of FLAG-DAXX used in (*B*). *B*, coimmunoprecipitation analysis of ZFAT-HA and the deletion mutants of FLAG-DAXX in HEK293 cells using anti-HA and anti-FLAG antibodies. The data are representative of three independent experiments. DAXX, death domain–associated protein; FLAG-DAXX, FLAG-tagged DAXX; HA, hemagglutinin; HEK293, human embryonic kidney 293 cell line; ZFAT, zinc-finger protein with AT hook; ZFAT-HA, hemagglutinin-tagged ZFAT; WCL, whole cell lysate.

localization of ZFAT specifically at the centromeres but not at the gene promoter regions.

To further examine the involvement of DAXX in the centromeric localization of ZFAT, we next evaluated the effect of loss of the endogenous DAXX protein on the centromeric ZFAT levels in HEK293 cells transiently expressing ZFAT-HA (Figs. 5, *A* and *B*, and S1*A* and *B*). We used two siRNAs (siDAXX-1 and siDAXX-2) targeting distinct sequences of DAXX to deplete the DAXX protein. Transfection of cells with siRNAs for DAXX significantly decreased the expression levels of endogenous DAXX protein but not those of ectopically expressed ZFAT-HA (Figs. 5*A* and S1*A*). Loss of DAXX resulted in the significant decrease in the protein levels of ZFAT at the centromeres, compared with a control siRNA (Figs. 5*B* and S1*B*). On the other hand, the DAXX siRNAs did not affect the protein levels of ZFAT at the promoter regions of the *BRPF1*, *PDE12*, and *TELO2* genes (Figs. 5, *B* and *C*, and S1*B*). Together, these results suggest that DAXX promotes the localization of ZFAT specifically at the centromeres.

DAXX is involved in ZFAT-regulated ncRNA transcription at the centromeres

To investigate the involvement of DAXX in ZFAT-regulated centromeric ncRNA transcription, we examined the effects of ectopic expression of ZFAT-HA, FLAG-DAXX, or both on the centromeric ncRNA levels in HEK293 cells (Fig. 6, *A* and *B*). The expression levels of centromeric ncRNA were determined by qRT–PCR analysis, which we established previously (11, 12). As previously shown (12), ectopic expression of ZFAT alone caused a marked increase in the centromeric ncRNA levels but not in the RNA expression levels of the Alu element that was noncentromeric repetitive DNA sequence (Fig. 6*B*). Interestingly, ectopic coexpression of ZFAT with DAXX resulted in a further increase in the centromeric ncRNA levels, compared with those in cells expressing ZFAT alone (Fig. 6*B*). Furthermore, DAXX, which was ectopically expressed alone, slightly increased the centromeric ncRNA levels although it was not statistically significant (Fig. 6*B*). These results suggest that DAXX plays positive roles in ZFAT-regulated centromeric ncRNA transcription.

We next evaluated the effects of loss of endogenous DAXX protein on the centromeric ncRNA levels in HEK293 cells transiently expressing ZFAT-HA (Figs. 7, *A* and *B*, and S1*C*). siRNA-mediated knockdown of DAXX significantly decreased the centromeric ncRNA levels in cells expressing ZFAT-HA, compared with a control siRNA (Figs. 7*B* and S1*C*). Together, these results suggest that DAXX is involved in ZFAT-regulated ncRNA transcription at the centromeres.

DAXX is required for the ZFAT-regulated centromeric ncRNA transcription and accurate chromosomal segregation

To further elucidate the role of DAXX in the ZFAT-regulated ncRNA transcription at the centromeres, we evaluated the effects of DAXX depletion on the centromeric ncRNA levels in HEK293 cells without ectopic expression of ZFAT-HA (Figs. 8, *A* and *B*, and S2*A* and *B*). An siRNA-mediated knockdown of DAXX had no effects on the expression levels of endogenous ZFAT protein (Figs. 8*B* and S2*B*). A depletion of DAXX caused a significant decrease in the ncRNA levels at the centromeres of chromosomes 17 and X in which ZFAT regulated the transcription (Figs. 8*A* and S2*A*). These results suggest that DAXX is involved in the ZFAT-regulated centromeric ncRNA transcription at a physiological state.

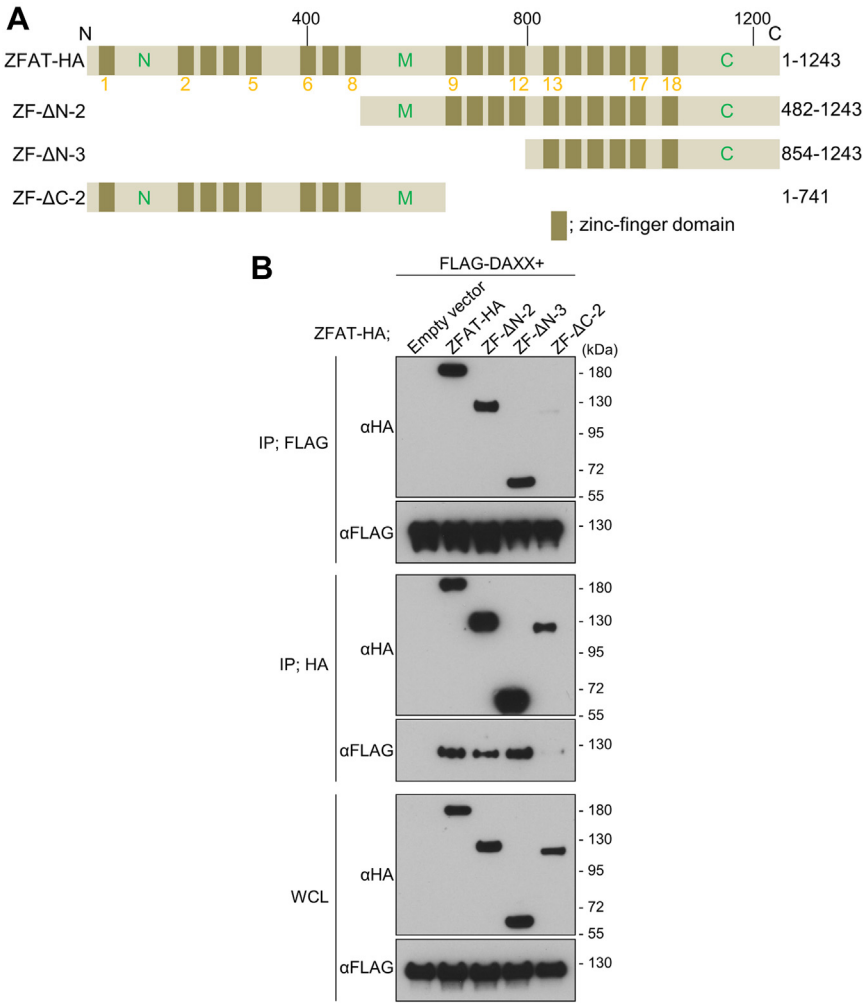

Figure 3. The C-terminal domain of ZFAT interacts with DAXX. *A*, schematic diagram of the deletion mutants of ZFAT-HA used in (*B*). *B*, coimmunoprecipitation analysis of FLAG-DAXX and the deletion mutants of ZFAT-HA in HEK293 cells using anti-HA and anti-FLAG antibodies. The data are representative of three independent experiments. DAXX, death domain–associated protein; FLAG-DAXX, FLAG-tagged DAXX; HA, hemagglutinin; HEK293, human embryonic kidney 293 cell line; WCL, whole cell lysate; ZFAT, zinc-finger protein with AT hook; ZFAT-HA, hemagglutinin-tagged ZFAT.

Transcription at the centromeres and its ncRNA products are important for centromere functions in accurate chromosomal segregation. We next examined the effects of DAXX depletion on formation of mitotic spindle using immunofluorescence analysis of α-tubulin (Figs. 8, *C* and *D* and S2*C* and *D*). In these experiments, we used HT1080 cells, which were near diploid cells, instead of HEK293 cells, because abnormal spindle morphology was frequently observed in HEK293 cells without any treatments. Depletion of DAXX significantly increased the proportion of mitotic cells that had abnormal spindle morphology, compared with cells transfected with a control siRNA (Fig. 8, *C* and *D* and S2*C* and *D*). Together, these results suggest that DAXX is involved in the accurate chromosome segregation probably through the ZFAT-regulated centromeric ncRNA transcription.

Discussion

DAXX was previously reported to localize at the centromeres in human cells (39). Furthermore, Morozov *et al.* (38) reported that depletion of DAXX resulted in decreases in the centromeric levels of both ncRNA and the histone H3 variant H3.3. It was also shown that DAXX-mediated deposition of H3.3 was related to the activation of ncRNA transcription in pericentromeric regions in mouse cells (37). These previous studies have together suggested that DAXX is involved in ncRNA transcription at the centromeres by facilitating the deposition of H3.3. However, heat shock treatment of human cells caused marked increases in the centromeric levels of DAXX, but not ncRNA, indicating that the DAXX levels at the centromeres are not completely correlated to the centromeric ncRNA levels (38). Thus, mechanisms by which DAXX regulates ncRNA transcription at the centromeres remain elusive. In this study, we identified the transcription regulator ZFAT as a novel interacting protein of DAXX (Figs. 1–3). Furthermore, we showed that the protein levels of DAXX were obviously correlated to the centromeric levels of both ZFAT and ncRNA (Figs. 4–7). These results demonstrate that DAXX regulates ncRNA transcription at the centromeres, at least in part, through

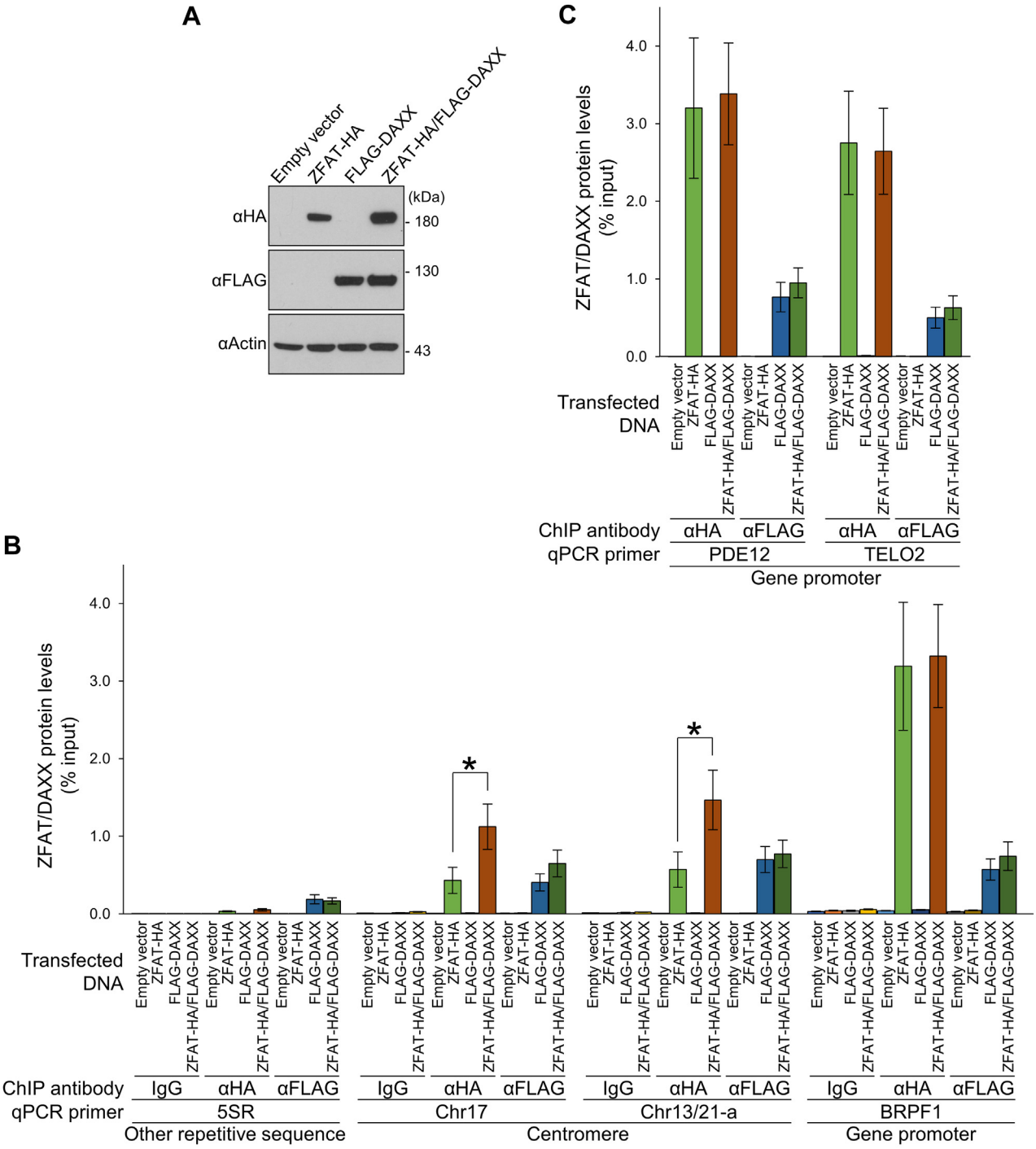

Figure 4. Coexpression of DAXX and ZFAT increases the ZFAT protein levels at the centromeres. *A*, immunoblotting analysis of ZFAT-HA and FLAG-DAXX using anti-HA and anti-FLAG antibodies in HEK293 cells transfected with the indicated expression vectors. Actin was used as a loading control. The data are representative of three independent experiments. *B* and *C*, ChIP–qPCR analysis of ZFAT-HA and FLAG-DAXX at the human repetitive DNA sequences and the gene promoter regions using anti-HA and anti-FLAG antibodies or control immunoglobulin G (IgG) in HEK293 cells transfected with the indicated expression vectors. The data represent the mean ± SD of three independent experiments. *$p < 0.05$. ChIP, chromatin immunoprecipitation; DAXX, death domain–associated protein; FLAG-DAXX, FLAG-tagged DAXX; HA, hemagglutinin; HEK293, human embryonic kidney 293 cell line; qPCR, quantitative PCR; ZFAT, zinc-finger protein with AT hook; ZFAT-HA, hemagglutinin-tagged ZFAT.

interaction with ZFAT. Taken together, we propose that DAXX plays crucial roles in centromeric ncRNA transcription through both deposition of H3.3 and localization of ZFAT (Fig. 8*E*).

We have recently reported that the centromeric protein CENP-B interacts with ZFAT to promote the centromeric localization of ZFAT (11). Interestingly, it was also previously reported that CENP-B interacted with DAXX (40). Depletion of CENP-B decreases the centromeric levels of DAXX, indicating that CENP-B is required for the centromeric localization of DAXX (40). In this study, we showed that the C-terminal region of ZFAT was involved in the interaction

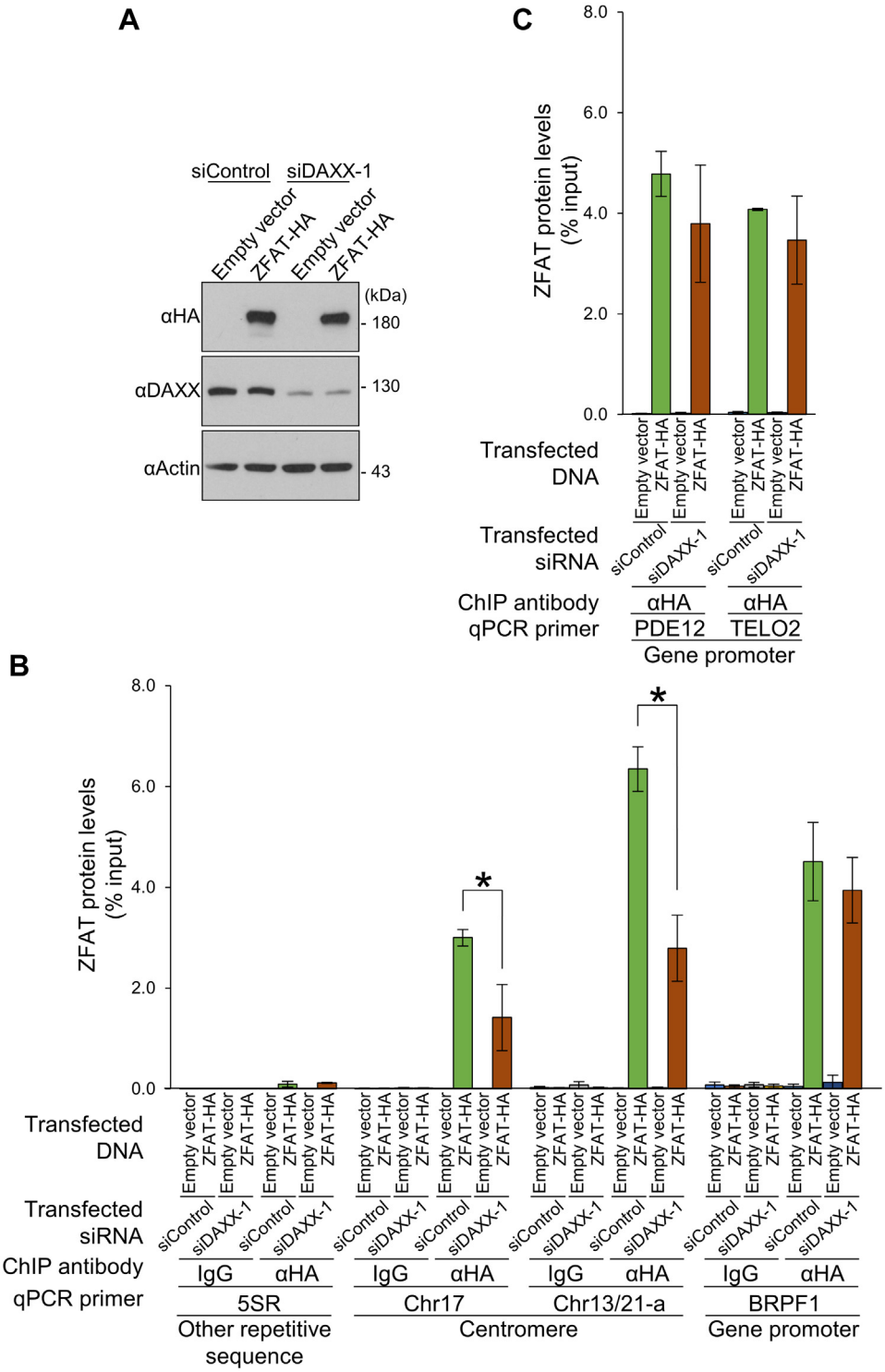

Figure 5. Loss of DAXX decreases the ZFAT protein levels at the centromeres. *A*, immunoblotting analysis of ZFAT-HA and endogenous DAXX proteins using anti-HA and anti-DAXX antibodies in HEK293 cells transfected with the indicated expression vectors and siRNAs for control (siControl) or DAXX (siDAXX-1). Actin was used as a loading control. The data are representative of three independent experiments. *B* and *C*, ChIP–qPCR analysis of ZFAT-HA at the human repetitive DNA sequences and the gene promoter regions using an anti-HA antibody or control immunoglobulin G (IgG) in HEK293 cells transfected with the indicated expression vectors, and siControl or siDAXX-1. The data represent the mean ± SD of three independent experiments. *$p < 0.05$. ChIP, chromatin immunoprecipitation; DAXX, death domain–associated protein; HA, hemagglutinin; HEK293, human embryonic kidney 293 cell line; qPCR, quantitative PCR; ZFAT, zinc-finger protein with AT hook; ZFAT-HA, hemagglutinin-tagged ZFAT.

with DAXX (Fig. 3). On the other hand, we previously showed that the middle domain of ZFAT was required for the interaction with CENP-B (11). Thus, ZFAT separately interacts with DAXX and CENP-B through distinct regions. A ternary complex of CENP-B, DAXX, and ZFAT would play important roles in ncRNA transcription at the centromeres (Fig. 8*E*).

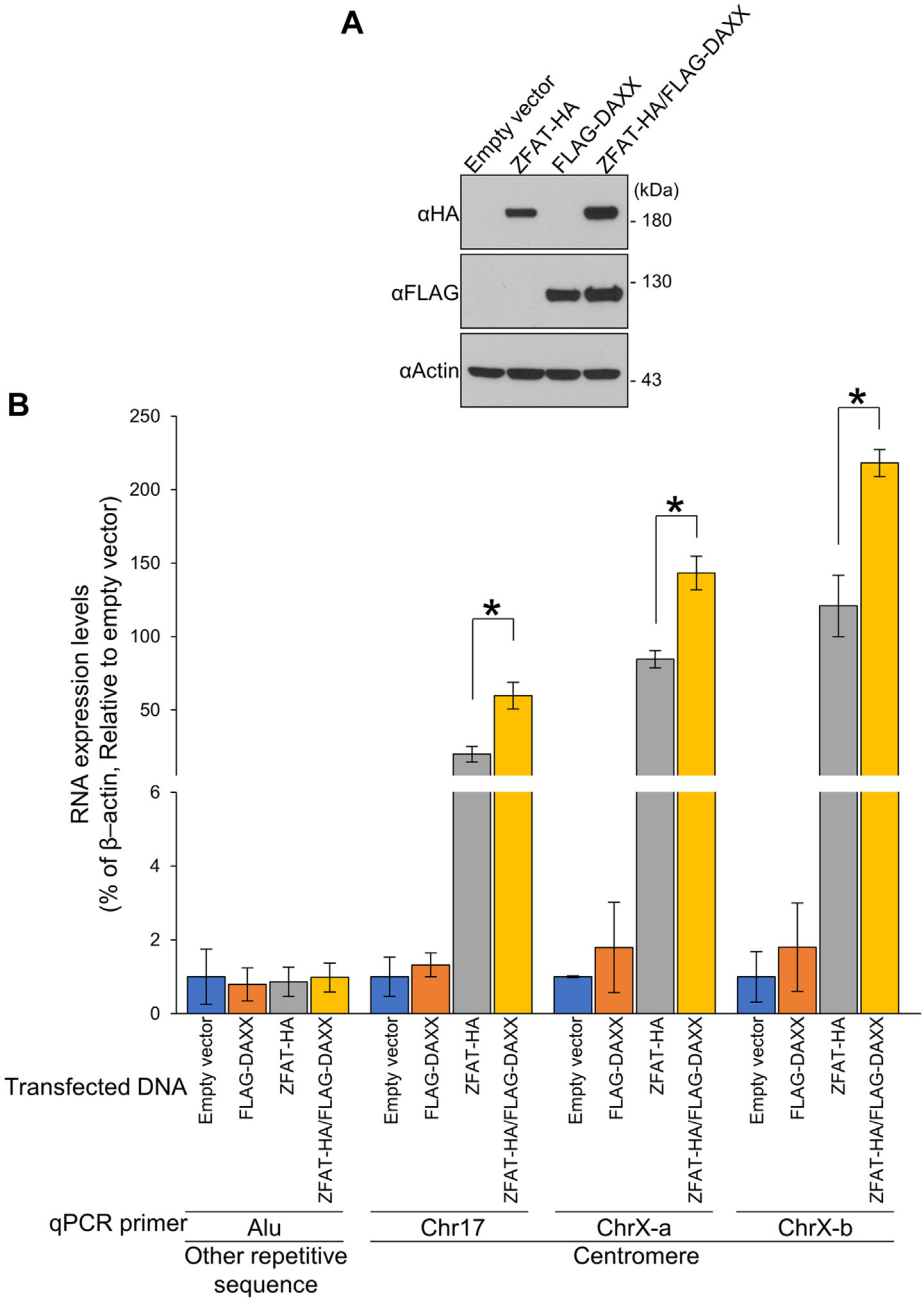

Figure 6. Coexpression of DAXX and ZFAT stimulates the ZFAT-regulated ncRNA transcription at the centromeres. *A*, immunoblotting analysis of ZFAT-HA and FLAG-DAXX using anti-HA and anti-FLAG antibodies in HEK293 cells transfected with the indicated expression vectors. Actin was used as a loading control. The data are representative of three independent experiments. *B*, qRT–PCR analysis of RNA derived from human repetitive sequences in HEK293 cells transfected with the indicated expression vectors. The RNA expression levels were shown as the relative values to those in cells transfected with an empty vector. The data represent the mean ± SD of three independent experiments. *$p < 0.05$. DAXX, death domain–associated protein; FLAG-DAXX, FLAG-tagged DAXX; HA, hemagglutinin; HEK293, human embryonic kidney 293 cell line; ncRNA, noncoding RNA; qRT–PCR, quantitative RT–PCR; ZFAT, zinc-finger protein with AT hook; ZFAT-HA, hemagglutinin-tagged ZFAT.

In this study, we showed that the ZFAT protein levels at the centromeres relied on the presence of the DAXX protein (Figs. 4 and 5). Furthermore, evident interaction between ZFAT and DAXX was observed in human cells (Figs. 1–3). On the other hand, we have previously shown that ZFAT binds directly to the centromeric DNA with specific DNA sequences (12), indicating that ZFAT would not bind to the centromeric DNA through the DAXX protein. Thus, DAXX may contribute to the centromeric localization of ZFAT through stabilization of the binding of ZFAT to the centromeric DNA, cooperatively with CENP-B (Fig. 8*E*).

Here, we showed that loss of DAXX resulted in the decreased centromeric ncRNA levels as well as abnormal spindle morphology (Fig. 8). Centromeric ncRNA transcription plays important roles in centromere functions, and its dysregulation causes chromosome segregation error, leading to aneuploidy, which is one of the representative characteristics of tumor cells. Indeed, aberrant expression of centromeric

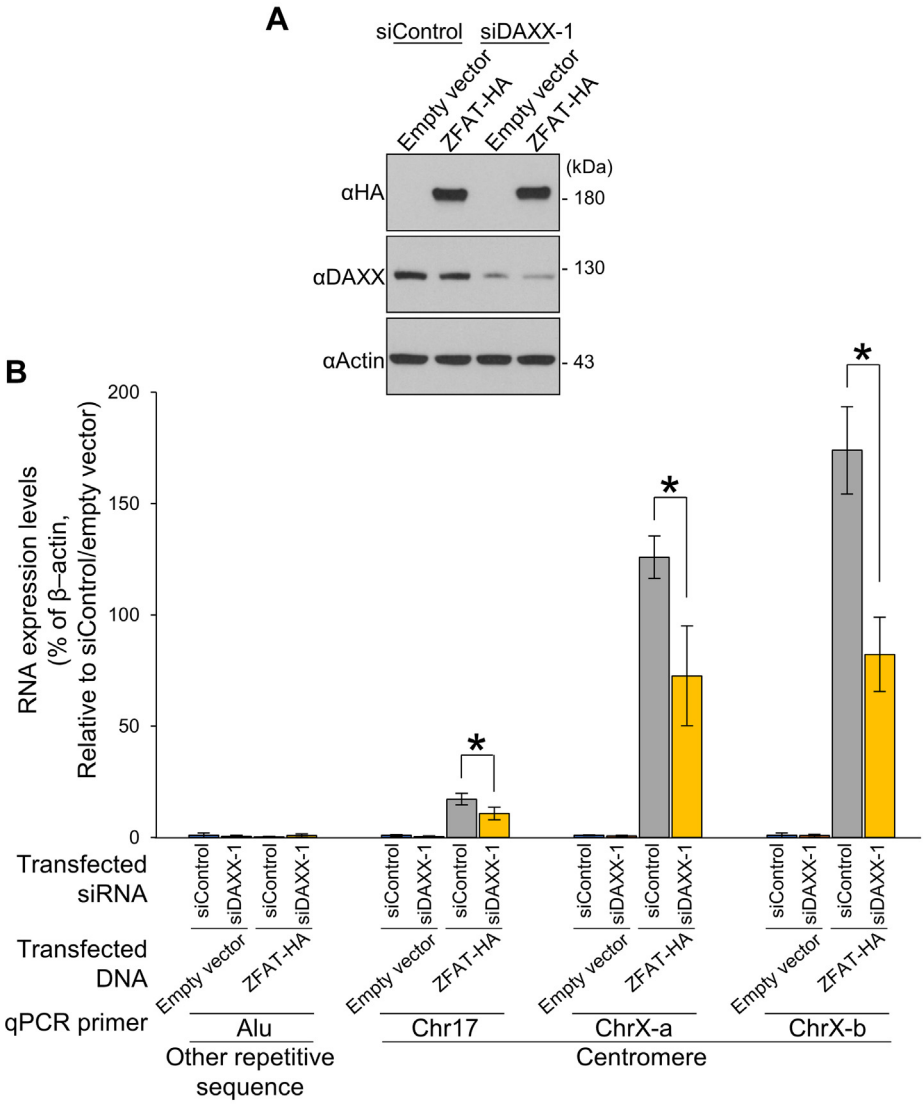

Figure 7. Loss of DAXX inhibits the ZFAT-regulated ncRNA transcription at the centromeres. *A*, immunoblotting analysis of ZFAT-HA and endogenous DAXX proteins using anti-HA and anti-DAXX antibodies in HEK293 cells transfected with the indicated expression vectors and siRNAs for control (siControl) or DAXX (siDAXX-1). Actin was used as a loading control. The data are representative of three independent experiments. *B*, qRT–PCR analysis of RNA derived from human repetitive sequences in HEK293 cells transfected with the indicated expression vectors and siControl or siDAXX-1. The RNA expression levels were shown as the relative values to those in cells transfected with an empty vector and siControl. The data represent the mean ± SD of three independent experiments. *$p < 0.05$. DAXX, death domain–associated protein; HEK293, human embryonic kidney 293 cell line; ncRNA, noncoding RNA; qRT–PCR, quantitative RT–PCR; ZFAT, zinc-finger protein with AT hook; ZFAT-HA, hemagglutinin-tagged ZFAT.

ncRNA is observed in several human cancer tissues (41, 42). Interestingly, mutations and altered expression of DAXX are observed in diverse human cancers. Given that ectopic expression of DAXX alone resulted in a slight increase in the centromeric ncRNA levels (Fig. 6*B*), the activation of the ZFAT-regulated centromeric transcription may be related to the tumorigenicity by an increased expression of DAXX in cancer cells.

On the other hand, roles of DAXX in tumorigenesis are different in diverse cancers. For example, DAXX is overexpressed in ovarian cancer tissues and promotes the development of ovarian tumors (43). On the other hand, it was recently reported that DAXX functions as a suppressor for epithelial–mesenchymal transition and invasion of lung cancer cells through interaction with the ZF transcription factor Slug (44). Thus, roles of DAXX in cancer cells are dependent on the cellular contexts and gene expression profiles of cells, suggesting that the expression levels and/or mutations of DAXX-interacting partners may determine roles of DAXX in cancer cells. Interestingly, mutations in the *ZFAT* gene have also been found in several human cancers (25–28, 30, 31). Furthermore, overexpression of ZFAT is observed in ovarian cancer (29). Therefore, impaired centromeric transcription caused by simultaneous dysregulation of ZFAT and DAXX may be cooperatively involved in development and progression of cancer cells, including ovarian cancer.

We have previously shown that percentages of mitotic cells with abnormal spindle morphology in ZFAT-depleted cells are 84% and 74% using two distinct siRNAs (12). In contrast, those in DAXX-depleted cells were 67% and 74%, as shown in

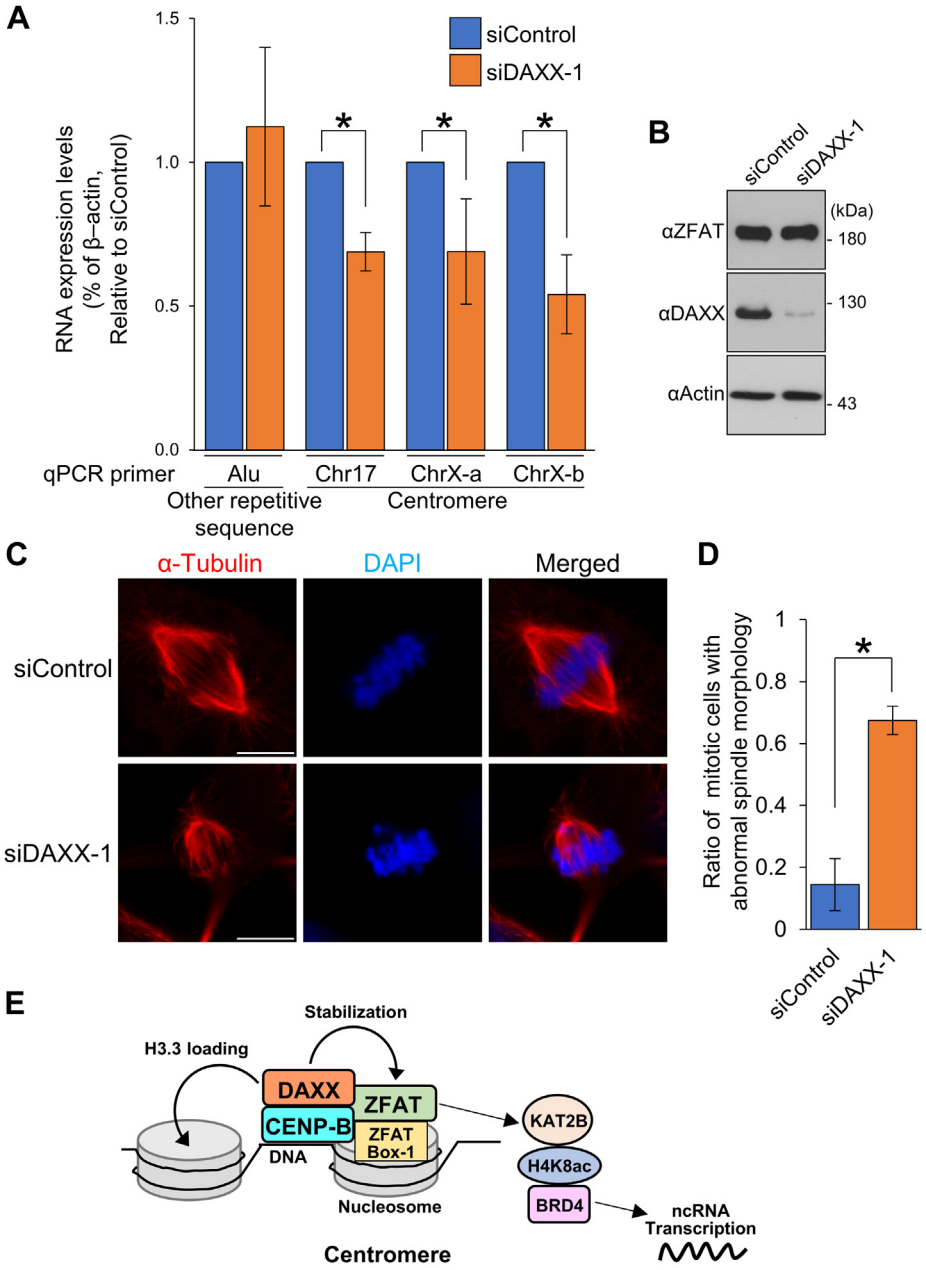

Figure 8. Loss of DAXX results in the decreased centromeric ncRNA levels and abnormal spindle morphology. *A*, qRT–PCR analysis of RNA derived from human repetitive sequences in HEK293 cells transfected with siRNAs for control (siControl) or DAXX (siDAXX-1). The RNA expression levels were shown as the relative values to those in cells transfected with siControl. *B*, immunoblotting analysis of endogenous ZFAT and DAXX proteins using anti-ZFAT and anti-DAXX antibodies in HEK293 cells transfected with siControl or siDAXX-1. Actin was used as a loading control. *C*, representative immunofluorescence images of α-tubulin and DAPI in HT1080 cells transfected with siControl or siDAXX-1. The scale bar represents 5 μm. *D*, percentage of cells with an abnormal spindle morphology in mitotic cells transfected with siControl or siDAXX-1, determined in (*C*). N = 30 cells per one experiment. *E*, the model of the role of DAXX in the ncRNA transcription regulation at the centromeres. *A* and *D*, the data represent the mean ± SD of three independent experiments. *$p < 0.05$. *B* and *C*, the data are representative of three independent experiments. DAPI, 4′,6-diamidino-2-phenylindole; DAXX, death domain–associated protein; HEK293, human embryonic kidney 293 cell line; ncRNA, noncoding RNA; qRT–PCR, quantitative RT–PCR; ZFAT, zinc-finger protein with AT hook.

Figs. 8*D* and S2*D* in this study. These results are consistent with our conclusion that mitotic spindle defects observed in DAXX-depleted cells mainly result from the impaired centromeric localization of ZFAT. On the other hand, DAXX has been known to interact with various molecules that are involved in mitosis (45, 46). Thus, we cannot rule out the possibility that the abnormal spindle morphology observed in DAXX-depleted cells is unrelated with the ZFAT-regulated centromeric ncRNA transcription. Elucidating roles of DAXX through the centromeric ncRNA transcription in accurate chromosome segregation will be addressed in future studies.

In summary, our study elucidated the molecular mechanisms of centromeric ncRNA transcription regulated by DAXX. We identified ZFAT as a novel interacting protein of DAXX. The centromeric levels of ZFAT were correlated with the presence of DAXX. Furthermore, depletion of DAXX resulted in the decreased centromeric ncRNA levels and

abnormal spindle formation. Thus, we propose that DAXX controls ncRNA transcription at the centromeres through interaction with ZFAT. DAXX plays crucial roles in centromeric ncRNA transcription through both deposition of H3.3 and localization of ZFAT. These findings would lead to a better understanding of functional significance of DAXX and ZFAT in cell survival and death as well as tumorigenesis.

Experimental procedures

Cell culture

The cell lines HEK293 and HT1080 were cultured at 37 °C with 5% CO_2 in Dulbecco's modified Eagle's medium (Wako Pure Chemical Industries; catalog no.: 041-30081) and supplemented with 10% fetal bovine serum and penicillin/streptomycin (Gibco; catalog no.: 15140122).

Constructs

The constructs and primers used in this study are detailed in Tables S1 and S2, respectively. The expression vectors for human ZFAT and CENP-B have been previously described (11, 12). Complementary DNA for human DAXX was obtained from Addgene (#119021) and cloned into pcDNA3 plasmid DNA for expression in cultured mammalian cells. The expression vectors were verified by DNA sequencing.

Immunoblotting and co-IP

The immunoblotting procedure was performed as previously described using antibodies detailed in Table S3 (11, 15, 47). co-IP was performed in HEK293 cells as previously described (12, 48). Briefly, HEK293 cells were lysed in co-IP buffer (50 mM Tris–HCl, pH 7.5; 150 mM NaCl; 5 mM $MgCl_2$; 10% glycerol; and 1% NP-40) supplemented with cOmplete EDTA-Free Protease Inhibitor (Sigma–Aldrich) by incubation for 30 min at 4 °C. Cell pellets were removed by centrifugation, and the supernatants were precleaned by incubation with rat, mouse, or rabbit immunoglobulin G and Protein G Sepharose (GE Healthcare Life Sciences) for 30 min at 4 °C under gentle rotation. After centrifugation, the supernatants were coimmunoprecipitated by incubation with primary antibodies (Table S3) conjugated with Protein G Sepharose at 4 °C under gentle rotation overnight. The beads were washed with co-IP buffer three times and then boiled in Laemmli sample buffer. The eluates were subjected to immunoblotting.

To treat lysates with DNase before co-IP, cells were lysed in co-IP buffer for DNase (50 mM Tris–HCl, pH 8; 150 mM NaCl; 60 mM $MgCl_2$; 10 mM $CaCl_2$; 10% glycerol; and 1% NP-40) by incubation for 30 min at 4 °C. Cell pellets were removed by centrifugation, and supernatants were treated with 100 units/ml of DNase (Roche; catalog no.: 04716728001) for 15 min at 37 °C, and then co-IP was performed.

siRNA transfection

The siRNA against DAXX was purchased from Thermo Fisher Scientific (siDAXX-1, DAXXHSS175936, 5′-GAUCAUCGUGCUCUCAGACUCUGAU-3′; siDAXX-2, DAXXHSS175937, 5′-AGCAGUAGUUCGGGCGGCAAGAAAU). HEK293 cells were transfected with siRNA using Lipofectamine RNAiMAX (Invitrogen; catalog no.: 13778150) according to the manufacturer's reverse transfection protocol. Briefly, cells were seeded with siRNA (20 pmol)–Lipofectamine RNAiMAX (5 μl) complexes in 6-well plates at a density of 4×10^5 cells per well. After 24 h, the cells were transfected with plasmid DNA using Lipofectamine 3000 (Invitrogen; catalog no.: L3000015) and incubated for a further 24 h. Following incubation, the cells were utilized for downstream analyses.

ChIP–qPCR

ChIP–qPCR analysis was performed as previously described (12, 15). The antibodies and primers used in ChIP and qPCR are detailed in Tables S2 and S3. For ChIP–qPCR analysis of ZFAT-HA and FLAG-DAXX using anti-HA and anti-FLAG antibodies, HEK293 cells were transfected with the expression vectors using Lipofectamine 3000. After 24 h, the cells were crosslinked with 1% formaldehyde, lysed in radioimmunoprecipitation assay (RIPA) buffer (50 mM Tris–HCl, pH 8.0; 150 mM NaCl; 1% Triton X-100; 0.5% sodium deoxycholate; 0.1% SDS), and sonicated using a Bioruptor (Cosmo Bio) for 15 cycles at 1 min with 30 s on/off. After the ChIP procedure, the beads were serially washed with either RIPA, RIPA containing 500 mM NaCl, and RIPA containing 250 mM LiCl and TE buffers (10 mM Tris–HCl, pH 8.0, 1 mM EDTA). qPCR was performed using TB Green Premix Ex Taq GC (Perfect Real Time) (Takara Bio; catalog no.: RR071B) with 7500 Fast Real-Time PCR system (Applied Biosystems). Results of ChIP–qPCR analysis are represented as the percentage (%) of input, which represents the amount of DNA pulled down by using an antibody for HA or FLAG tag in the ChIP reaction, relative to the amount of genome DNA used. The amount of pulled down DNA is normalized to the number of their binding sites in the whole genome.

qRT–PCR

qRT–PCR analysis was performed as previously described (11, 12, 48). For those HEK293 cells that were transfected with siRNA against DAXX using RNAiMAX for 72 h, the total RNA was extracted using TRIZol reagent (Invitrogen; catalog no.: 15596018). Complementary DNA was synthesized using the ReverTra Ace qPCR RT Master Mix with gDNA Remover (Toyobo; catalog no.: FSQ-301). Control samples without reverse transcriptase were performed to identify DNA contamination. qPCR was performed using the Thunderbird SYBR qPCR Mix (Toyobo; catalog no.: QPX-201) with 7500 Fast Real-Time PCR system according to the manufacturer's instructions. The primers used for qPCR are detailed in Table S2.

Immunofluorescence microscopy

Immunofluorescence analysis was performed as previously described (11, 12). HT1080 cells were seeded with siRNA

(5 pmol)–Lipofectamine RNAiMAX (1.25 μl) complexes onto a 12 mm diameter glass coverslip and placed into 24-well plates. After 72 h, the transfected cells were fixed with 100% methanol for 20 min at −20 °C, subsequently washed thrice with PBS, permeabilized, and blocked with 5% fetal bovine serum in PBS containing 0.3% Triton X-100 for 30 min at room temperature, and subsequently incubated with an anti-α-tubulin antibody at 4 °C overnight. Following incubation, the cells were washed thrice with PBS and subsequently incubated with secondary antibodies conjugated with fluorescent dyes for 1 h at room temperature. Cells were then washed thrice with PBS, stained with 4′,6-diamidino-2-phenylindole, mounted using Fluorescence Mounting Medium (Dako; catalog no.: S3023), and viewed using a TCS SP5 laser-scanning confocal microscope (Leica Microsystems).

Statistical analysis

The data were expressed as the mean ± standard deviation. The statistical analyses were performed using an unpaired two-tailed Student's t test. A $p < 0.05$ denoted a statistically significant difference.

Data availability

All data are contained in the article or available on request by contacting the corresponding author: sshirasa@fukuoka-u.ac.jp.

Supporting information—This article contains Supporting information (12).

Author contributions—S. I. conceptualization; S. I. methodology; S. I., K. Y., and T. T. investigation; S. I. writing–original draft; K. Y., T. T., and S. S. writing–review & editing; S. S. supervision.

Funding information—This work was supported by Japan Society for the Promotion of Science KAKENHI grant (grant nos.: 20K07317 [to S. I.] and 22K07221 [to K. Y.]) and by funding from Fukuoka University (Grantgrant nos. 925 and K22009).

Conflict of interest—The authors declare that they have no conflicts of interest with the contents of this article.

Abbreviations—The abbreviations used are: AD, acidic domain; ChIP, chromatin immunoprecipitation; co-IP, coimmunoprecipitation; DAXX, death domain–associated protein; FLAG-CENP-B, FLAG-tagged CENP-B; FLAG-DAXX, FLAG-tagged DAXX; HA, hemagglutinin; HEK293, human embryonic kidney 293 cell line; ncRNA, noncoding RNA; qPCR, quantitative PCR; RIPA, radioimmunoprecipitation assay; SIM, SUMO-interacting motif; ZF, zinc finger; ZFAT, zinc-finger protein with AT hook; ZFAT-HA, hemagglutinin-tagged ZFAT.

References

1. McKinley, K. L., and Cheeseman, I. M. (2016) The molecular basis for centromere identity and function. *Nat. Rev. Mol. Cell Biol.* **17**, 16–29
2. Bouzinba-Segard, H., Guais, A., and Francastel, C. (2006) Accumulation of small murine minor satellite transcripts leads to impaired centromeric architecture and function. *Proc. Natl. Acad. Sci. U. S. A.* **103**, 8709–8714
3. Chan, F. L., Marshall, O. J., Saffery, R., Kim, B. W., Earle, E., Choo, K. H., *et al.* (2012) Active transcription and essential role of RNA polymerase II at the centromere during mitosis. *Proc. Natl. Acad. Sci. U. S. A.* **109**, 1979–1984
4. Hoyt, S. J., Storer, J. M., Hartley, G. A., Grady, P. G. S., Gershman, A., de Lima, L. G., *et al.* (2022) From telomere to telomere: the transcriptional and epigenetic state of human repeat elements. *Science* **376**, eabk3112
5. Quenet, D., and Dalal, Y. (2014) A long non-coding RNA is required for targeting centromeric protein A to the human centromere. *Elife* **3**, e03254
6. Topp, C. N., Zhong, C. X., and Dawe, R. K. (2004) Centromere-encoded RNAs are integral components of the maize kinetochore. *Proc. Natl. Acad. Sci. U. S. A.* **101**, 15986–15991
7. Chen, Y., Zhang, Q., and Liu, H. (2022) An emerging role of transcription in chromosome segregation: ongoing centromeric transcription maintains centromeric cohesion. *Bioessays* **44**, e2100201
8. Mihic, P., Hedouin, S., and Francastel, C. (2021) Centromeres transcription and transcripts for better and for worse. *Prog. Mol. Subcell Biol.* **60**, 169–201
9. Liu, Q., Liu, Y., Shi, Q., Su, H., Wang, C., Birchler, J. A., *et al.* (2021) Emerging roles of centromeric RNAs in centromere formation and function. *Genes Genomics* **43**, 217–226
10. Leclerc, S., and Kitagawa, K. (2021) The role of human centromeric RNA in chromosome stability. *Front Mol. Biosci.* **8**, 642732
11. Ishikura, S., Yoshida, K., Hashimoto, S., Nakabayashi, K., Tsunoda, T., and Shirasawa, S. (2021) CENP-B promotes the centromeric localization of ZFAT to control transcription of noncoding RNA. *J. Biol. Chem.* **297**, 101213
12. Ishikura, S., Nakabayashi, K., Nagai, M., Tsunoda, T., and Shirasawa, S. (2020) ZFAT binds to centromeres to control noncoding RNA transcription through the KAT2B-H4K8ac-BRD4 axis. *Nucleic Acids Res.* **48**, 10848–10866
13. Tochio, N., Umehara, T., Nakabayashi, K., Yoneyama, M., Tsuda, K., Shirouzu, M., *et al.* (2015) Solution structures of the DNA-binding domains of immune-related zinc-finger protein ZFAT. *J. Struct. Funct. Genomics* **16**, 55–65
14. Tsunoda, T., Doi, K., Ishikura, S., Luo, H., Nishi, K., Matsuzaki, H., *et al.* (2018) Zfat expression in ZsGreen reporter gene knockin mice: implications for a novel function of Zfat in definitive erythropoiesis. *Int. J. Mol. Med.* **42**, 2595–2603
15. Ishikura, S., Tsunoda, T., Nakabayashi, K., Doi, K., Koyanagi, M., Hayashi, K., *et al.* (2016) Molecular mechanisms of transcriptional regulation by the nuclear zinc-finger protein Zfat in T cells. *Biochim. Biophys. Acta* **1859**, 1398–1410
16. Ishikura, S., Iwaihara, Y., Tanaka, Y., Luo, H., Nishi, K., Doi, K., *et al.* (2016) The nuclear zinc finger protein Zfat maintains FoxO1 protein levels in peripheral T cells by regulating the activities of autophagy and the Akt signaling pathway. *J. Biol. Chem.* **291**, 15282–15291
17. Iwaihara, Y., Ishikura, S., Doi, K., Tsunoda, T., Fujimoto, T., Okamura, T., *et al.* (2015) Marked reduction in FoxO1 protein by its enhanced proteasomal degradation in Zfat-deficient peripheral T-cells. *Anticancer Res.* **35**, 4419–4423
18. Ishikura, S., Ogawa, M., Doi, K., Matsuzaki, H., Iwaihara, Y., Tanaka, Y., *et al.* (2015) Zfat-deficient CD4(+) CD8(+) double-positive thymocytes are susceptible to apoptosis with deregulated activation of p38 and JNK. *J. Cell Biochem.* **116**, 149–157
19. Ogawa, M., Okamura, T., Ishikura, S., Doi, K., Matsuzaki, H., Tanaka, Y., *et al.* (2013) Zfat-deficiency results in a loss of CD3zeta phosphorylation with dysregulation of ERK and Egr activities leading to impaired positive selection. *PLoS One* **8**, e76254
20. Inoue, N., Watanabe, M., Yamada, H., Takemura, K., Hayashi, F., Yamakawa, N., *et al.* (2012) Associations between autoimmune thyroid disease prognosis and functional polymorphisms of susceptibility genes, CTLA4, PTPN22, CD40, FCRL3, and ZFAT, previously revealed in genome-wide association studies. *J. Clin. Immunol.* **32**, 1243–1252
21. Shirasawa, S., Harada, H., Furugaki, K., Akamizu, T., Ishikawa, N., Ito, K., *et al.* (2004) SNPs in the promoter of a B cell-specific antisense transcript,

SAS-ZFAT, determine susceptibility to autoimmune thyroid disease. *Hum. Mol. Genet.* **13**, 2221–2231
22. Sabatino, G., Rigante, L., Minella, D., Novelli, G., Della Pepa, G. M., Esposito, G., *et al.* (2013) Transcriptional profile characterization for the identification of peripheral blood biomarkers in patients with cerebral aneurysms. *J. Biol. Regul. Homeost Agents* **27**, 729–738
23. Slavin, T. P., Feng, T., Schnell, A., Zhu, X., and Elston, R. C. (2011) Two-marker association tests yield new disease associations for coronary artery disease and hypertension. *Hum. Genet.* **130**, 725–733
24. Woo, H. J., and Reifman, J. (2018) Genetic interaction effects reveal lipid-metabolic and inflammatory pathways underlying common metabolic disease risks. *BMC Med. Genomics* **11**, 54
25. Catalano, C., Paramasivam, N., Blocka, J., Giangiobbe, S., Huhn, S., Schlesner, M., *et al.* (2021) Characterization of rare germline variants in familial multiple myeloma. *Blood Cancer J.* **11**, 33
26. de Araujo, E., Marchi, F. A., Rodrigues, T. C., Vieira, H. C., Kuasne, H., Achatz, M. I., *et al.* (2014) Genome-wide DNA methylation profile of leukocytes from melanoma patients with and without CDKN2A mutations. *Exp. Mol. Pathol.* **97**, 425–432
27. Erdogan, O. S., Tuncer, S. B., Kilic, S., Odemis, D. A., Turkcan, G. K., Celik, B., *et al.* (2020) Genome-wide methylation profiles in monozygotic twins with discordance for ovarian carcinoma. *Oncol. Lett.* **20**, 357
28. Gunnarsson, R., Yang, M., Olsson-Arvidsson, L., Biloglav, A., Behrendtz, M., Castor, A., *et al.* (2021) Single base substitution mutational signatures in pediatric acute myeloid leukemia based on whole genome sequencing. *Leukemia* **35**, 1485–1489
29. Ramakrishna, M., Williams, L. H., Boyle, S. E., Bearfoot, J. L., Sridhar, A., Speed, T. P., *et al.* (2010) Identification of candidate growth promoting genes in ovarian cancer through integrated copy number and expression analysis. *PLoS One* **5**, e9983
30. Zhang, F., Ruan, X., Ma, J., Liu, X., Zheng, J., Liu, Y., *et al.* (2020) DGCR8/ZFAT-AS1 promotes CDX2 transcription in a PRC2 complex-dependent manner to facilitate the malignant biological behavior of glioma cells. *Mol. Ther.* **28**, 613–630
31. Reddy, A., Zhang, J., Davis, N. S., Moffitt, A. B., Love, C. L., Waldrop, A., *et al.* (2017) Genetic and functional drivers of diffuse large B cell lymphoma. *Cell* **171**, 481–494.e15
32. Mahmud, I., and Liao, D. (2019) DAXX in cancer: Phenomena, processes, mechanisms and regulation. *Nucleic Acids Res.* **47**, 7734–7752
33. Gostissa, M., Morelli, M., Mantovani, F., Guida, E., Piazza, S., Collavin, L., *et al.* (2004) The transcriptional repressor hDaxx potentiates p53-dependent apoptosis. *J. Biol. Chem.* **279**, 48013–48023
34. Emelyanov, A. V., Kovac, C. R., Sepulveda, M. A., and Birshtein, B. K. (2002) The interaction of Pax5 (BSAP) with Daxx can result in transcriptional activation in B cells. *J. Biol. Chem.* **277**, 11156–11164
35. Kuo, H. Y., Chang, C. C., Jeng, J. C., Hu, H. M., Lin, D. Y., Maul, G. G., *et al.* (2005) SUMO modification negatively modulates the transcriptional activity of CREB-binding protein via the recruitment of Daxx. *Proc. Natl. Acad. Sci. U. S. A* **102**, 16973–16978
36. Hollenbach, A. D., McPherson, C. J., Mientjes, E. J., Iyengar, R., and Grosveld, G. (2002) Daxx and histone deacetylase II associate with chromatin through an interaction with core histones and the chromatin-associated protein Dek. *J. Cell Sci.* **115**, 3319–3330
37. Drane, P., Ouararhni, K., Depaux, A., Shuaib, M., and Hamiche, A. (2010) The death-associated protein DAXX is a novel histone chaperone involved in the replication-independent deposition of H3.3. *Genes Dev.* **24**, 1253–1265
38. Morozov, V. M., Gavrilova, E. V., Ogryzko, V. V., and Ishov, A. M. (2012) Dualistic function of Daxx at centromeric and pericentromeric heterochromatin in normal and stress conditions. *Nucleus* **3**, 276–285
39. Pluta, A. F., Earnshaw, W. C., and Goldberg, I. G. (1998) Interphase-specific association of intrinsic centromere protein CENP-C with HDaxx, a death domain-binding protein implicated in Fas-mediated cell death. *J. Cell Sci.* **111**, 2029–2041
40. Morozov, V. M., Giovinazzi, S., and Ishov, A. M. (2017) CENP-B protects centromere chromatin integrity by facilitating histone deposition via the H3.3-specific chaperone Daxx. *Epigenetics Chromatin* **10**, 63
41. Eymery, A., Horard, B., El Atifi-Borel, M., Fourel, G., Berger, F., Vitte, A. L., *et al.* (2009) A transcriptomic analysis of human centromeric and pericentric sequences in normal and tumor cells. *Nucleic Acids Res.* **37**, 6340–6354
42. Ting, D. T., Lipson, D., Paul, S., Brannigan, B. W., Akhavanfard, S., Coffman, E. J., *et al.* (2011) Aberrant overexpression of satellite repeats in pancreatic and other epithelial cancers. *Science* **331**, 593–596
43. Pan, W. W., Zhou, J. J., Liu, X. M., Xu, Y., Guo, L. J., Yu, C., *et al.* (2013) Death domain-associated protein DAXX promotes ovarian cancer development and chemoresistance. *J. Biol. Chem.* **288**, 13620–13630
44. Lin, C. W., Wang, L. K., Wang, S. P., Chang, Y. L., Wu, Y. Y., Chen, H. Y., *et al.* (2017) Corrigendum: daxx inhibits hypoxia-induced lung cancer cell metastasis by suppressing the HIF-1alpha/HDAC1/Slug axis. *Nat. Commun.* **8**, 14502
45. Giovinazzi, S., Lindsay, C. R., Morozov, V. M., Escobar-Cabrera, E., Summers, M. K., Han, H. S., *et al.* (2012) Regulation of mitosis and taxane response by Daxx and Rassf1. *Oncogene* **31**, 13–26
46. Giovinazzi, S., Morozov, V. M., Summers, M. K., Reinhold, W. C., and Ishov, A. M. (2013) USP7 and Daxx regulate mitosis progression and taxane sensitivity by affecting stability of Aurora-A kinase. *Cell Death Differ.* **20**, 721–731
47. Ishikura, S., Nagai, M., Tsunoda, T., Nishi, K., Tanaka, Y., Koyanagi, M., *et al.* (2021) The transcriptional regulator Zfat is essential for maintenance and differentiation of the adipocytes. *J. Cell Biochem.* **122**, 626–638
48. Nishi, K., Iwaihara, Y., Tsunoda, T., Doi, K., Sakata, T., Shirasawa, S., *et al.* (2017) ROS-induced cleavage of NHLRC2 by caspase-8 leads to apoptotic cell death in the HCT116 human colon cancer cell line. *Cell Death Dis.* **8**, 3218